

High-pressure high-temperature x-ray diffraction of β -boron to 30 GPaYanzhang Ma,¹ Charles T. Prewitt,² Guangtian Zou,³ Ho-kwang Mao,² and Russell J. Hemley²¹*Department of Mechanical Engineering, Texas Tech University, Lubbock, Texas 79409*²*Geophysical Laboratory, Carnegie Institution of Washington, 5251 Broad Branch Road N.W., Washington, DC 20015*³*National Laboratory of Superhard Materials, Jilin University, Changchun 130023, China*

(Received 3 December 2002; published 30 May 2003)

The high-pressure/high-temperature behavior of boron has been investigated up to 30 GPa using x-ray diffraction techniques. We have investigated the isothermal compressibility of rhombohedral-105 (*R*-105) boron to 30.7 GPa, and determined the bulk modulus K_{0T} to be $205(\pm 16)$ GPa with $K'_{0T}=4.3(\pm 1.6)$. We found that the *a* direction of *R*-105 boron (hexagonal setting) is less compressible than *c*, which indicates that the B10-B-B10 chain is less rigid than the B12 cluster. High *P-T* studies were conducted using double-sided laser heating to temperatures of 3500 K. *R*-105 boron transforms above 10 GPa at high temperature to a tetragonal phase that remains on *P-T* quenching. The transformation results in both a higher density and higher entropy phase and is consistent with the formation of the *T*-192 phase of boron.

DOI: 10.1103/PhysRevB.67.174116

PACS number(s): 81.40.Vw, 61.50.Ks, 64.30.+t, 81.30.-t

I. INTRODUCTION

The fact that boron is the first nonmetal solid element in the Periodic Table makes it an extraordinarily interesting topic in physics and chemistry. Twelve-atom clusters comprise pure boron and some boron-rich compounds, with each boron atom located on a vertex of an icosahedron. Boron has a characteristic electron-deficient nature (i.e., four bonding orbitals, but only three bonding electrons from each atom), and is proposed to form three-center valence bonds in establishing the icosahedral framework and two-center plus some three-center valence bonds linking the icosahedra.¹ The intericosahedral linkages have comparable strength with those of intra-icosahedra. Consequently, the icosahedral boron solids are not considered molecular solids although the 12-element cluster is the unifying motif under ambient pressure. Little is known about the comparative bond stability between the two sorts of bonds as well as the transformations of the basic structural units under extreme conditions.

Many previous studies of boron concentrated on the synthesis and structural characterization of pure forms. At least 15 crystalline forms as well as glass have been proposed or identified at different temperatures and/or fabrication conditions.² Only some of them have established crystal structures, whereas the rest are either characterized only by proposed diffraction indexing or simply by their reported diffraction patterns.² Numerous contradictions have arisen, including the proposal that only glassy boron, *R*-12, and *T*-192 boron exist for the pure element, whereas most of the previously reported crystal structures, including the most common β -boron (*B*-105), correspond to those of different borides.³ Hence, further investigations are necessary to resolve problems in the basic structural properties in this element. Problems also persist regarding reported high-pressure data for boron. Bridgman⁴ performed compressibility studies. Wentorf⁵ compressed boron in a multi-anvil apparatus to more than 10 GPa between 1500 and 2000 °C, and reported a 21 line x-ray diffraction pattern of the quenched sample (with the possibility of some sample impurities). Nelmes *et al.*⁶ employed neutron powder diffraction in a Paris-

Edinburgh cell and measured the bulk moduli of β -boron and used x-ray diffraction to examine α boron. Related studies of boron-rich solids suggested the possibility of “inverse” molecular compression,⁷ but this interpretation has been contested.⁸

Structural studies are also important for understanding other high-pressure data on boron. There have been questions regarding the interpretation of the vibrational spectrum. This has been addressed in a high-pressure study of the Raman spectrum by Vast *et al.*⁹ (see also references therein). Recently, the electrical conductivity was measured and showed discontinuities near 35 and 180 GPa, the latter corresponding to the transition to the superconducting state that persists to at least 250 GPa, where $T_c=11$ K (Ref. 10). The transformation is close to a theoretically predicted dissociation of the icosahedra.¹¹ However, there is no experimental information on the proposed structural changes.

Thus, we have little understanding of the structural behavior of boron at high pressure despite several decades of investigation. The main reason may mainly be ascribed to the complexity of the boron crystal structures themselves. As a low-*Z* element, boron has a very small x-ray scattering cross-section that renders these experiments difficult. The existence of a large number of borides and the problem of sample contamination further complicate the investigations. The utilization and development of intense synchrotron sources for x-ray diffraction in diamond anvil cells,¹² make it possible to undertake in situ high-pressure studies of bulk boron materials. In addition, the application of high power lasers to generate high temperatures in diamond cells provides us with a powerful tool to overcome kinetic barriers for driving high-pressure phase transformations. In this paper, we present an investigation of the stability of *R*-105 boron and high-pressure transformations through the use of synchrotron x-ray diffraction coupled with some newly developed sampling methods.

II. EXPERIMENTAL METHODS

Symmetrical diamond cells¹² with 300- μ m-culet diamonds were used in all of the experiments. Rhenium was

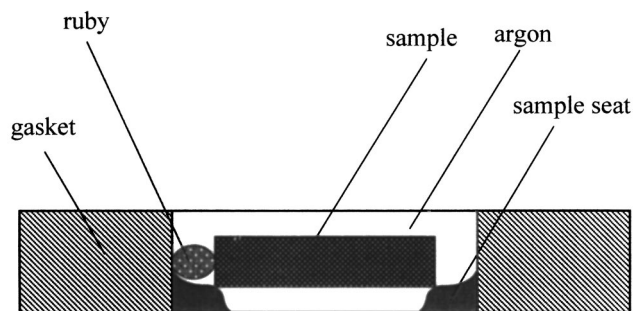


FIG. 1. Schematic diagram of the sample in a rhenium gasket with an argon pressure transmitting medium.

chosen as a gasket and 4:1 methanol and ethanol as pressure medium. The ruby fluorescence method was used for pressure calibration. A high purity boron sample (99.9999%, Alfa Aesar Co.) was confirmed by diffraction to have the $R-105$ structure, with $a = 10.91(\pm 3)$ Å, $c = 23.8(\pm 1)$ Å, $V = 2450(\pm 11)$ Å³, and $\rho = 2.307$ g cm⁻³, consistent with previous results.² Sample flakes with dimension of about 50 μm in diameter and 15 μm thick were obtained by aggregating material in a diamond cell. Diffraction patterns were taken to maximum pressure of 30.7 GPa in two separate runs to determine the equation of state and examine possible phase transitions at room temperature.

High P - T studies of boron were carried out using diamond cells described above together with a double-side laser heating technique.^{13,14} A high-power multimode YAG (yttrium aluminum garnet) laser was selected to generate a large uniform heating spot (50 μm). The laser beam was split into two parts by a 50/50 high-energy laser prism splitter, which was focused from both sides through the diamond on to the sample. The thermal emission was measured with a spectrometer/CCD detector system, from which temperatures were calculated. The heating was monitored visually with an optical microscope and camera. The gasket hole was 120 μm , which is sufficiently large in comparison to the x-ray beam to avoid diffraction by the gasket. To generate homogeneous heating conditions, NaCl and argon were used as both insulator and pressure media. In the runs with NaCl, two salt flakes of 5- μm thickness were placed on top of the two diamonds inside the gasket hole. For each experiment, 5- μm sized ruby chips were placed in the transparent part of the gasket hole far away from the sample to prevent their contact. The experiment with argon as the pressure medium was performed to compare the results with those obtained with the NaCl medium, including the possibility of reactions between boron and any residual gas (e.g., oxygen and nitrogen). In the argon runs, the sample was bridged by two small pieces (less than 10 μm) of the same boron at the bottom edge of the gasket hole to prevent sample contact with the diamonds before loading the argon (Fig. 1). The well-heated non-contact area was larger than 60 μm , a size that assured that x rays can distinguish the P - T processed region from the edge and the bridging piece of boron. In these experiments, the pressurized sample was first heated to temperatures ranging from 1500 to 3500 K on one spot; while maintaining constant heating conditions, the cell was then slowly trans-

lated to uniformly heat the entire sample. In this way high P - T processing under the same controlled conditions was achieved. After the sample was heated homogeneously, the laser was turned off and the sample quenched to room temperature. These temperature-quenched samples were examined by synchrotron x-ray diffraction both *in situ* and at ambient pressure. In the pressure-quenched experiment, NaCl was removed by a drop of water and the sample was held on a bamboo needle.

The experiments were mostly carried out at superconducting wiggler beam line X17C of the National Synchrotron Light Source (NSLS), Brookhaven National Laboratory. With the pairs of adjustable front slits and clean-up slits, a 200×200 - μm^2 x-ray beam for diffraction was reduced to dimensions as small as 15×20 μm^2 in our high temperature quenched sample measurements and 40×40 μm^2 in equation of state measurements. This produced a sharp, clean spatial distribution. This beam profiling is required for accurate probing of weak scattering samples located in the ~ 100 - μm gasket hole in the diamond cell. To overcome the effects of coarse graining of the sample and sample recrystallization during *in situ* high P - T experiments, a diamond-cell rotation technique was developed to allow a minimum angle resolution of 0.005° in a cell mounted on a high-precision, motor-driven rotation stage. This stage, together with the fine alignment of the cell, locates the sample to within less than a 5- μm error of the rotation center position within a 360° rotation. X rays collimated on the center of a vertical sample plane of ~ 50 μm in diameter can be accurately positioned on the sample during the stage rotation (χ rotation). To overcome effects of coarse crystallinity, we collected a diffraction pattern at each step of the χ rotation within a prescribed time limit. We could also continually rotate the cell while investigating phase transitions, especially for high-pressure melting point determination. This provides us with a diffraction versus χ -angle image, an image that contains the same information as that taken from an angle dispersive image plate. Coordinating the χ rotation with different 2θ within the opening cone of the rear cell seat, we could accurately map the whole diffracting cone space defined by the seat's opening. This method combines both the advantages of the intense x-ray source from an energy dispersive diffraction experiment and full spatial coverage of angle-dispersive diffraction. The most important advantage is that this method can accurately distinguish very weak diffraction peaks in a single pattern when the χ and 2θ angles are matched to the diffraction condition.¹⁵

Additional measurements were performed using monochromatic x-ray diffraction techniques at beamline C of the Cornell High Energy Synchrotron Source (CHESS). The Si(111) diffraction plane was chosen to generate a 0.495-Å monochromatic x-ray beam. A pinhole of 30 μm in diameter was used to confine the incident beam size and imaging plates used for detector. A very thin NaCl flake was placed on the bottom diamond of the cell and its diffraction lines were used to calibrate the sample to plate distance. Each sample examined was subjected to the same P - T conditions described above.

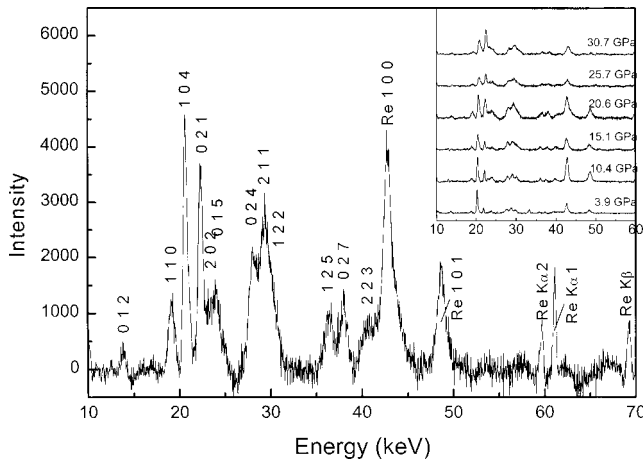


FIG. 2. X-ray diffraction pressure dependence of the (rhombohedral) β -boron. These patterns were taken without the step-rotation method; spectra were background corrected.

III. RESULTS AND DISCUSSION

A. Room-temperature equation of state

Figure 2 shows the diffraction pattern of boron measured as a function of pressure at room temperature. All major diffraction lines were found to shift continuously as a function of pressure. Figure 3 shows the P - V relations of β -boron to 30.7 GPa together with previous neutron data to 10 GPa. Fitting the P - V data to a Birch-Murnaghan equation of state yields a bulk modulus of $K_{0T}=205(\pm 16)$ GPa and $K'_{0T}=4.3(\pm 1.6)$; with fixed $K'_{0T}=4$; it yields $K_{0T}=208(\pm 3)$. The data are in good agreement with the neutron results⁶ within the error range. The larger covered pressure range is expected to provide a better constraint. Notably, the individual axial compressibilities differ. Figure 4 shows the pressure dependence of the lattice parameters of β -boron. Our data show that the a and c axes decrease by 1.3% and 2.2% at 10 GPa. Our fit gives a decrease in c/a of 0.09%/

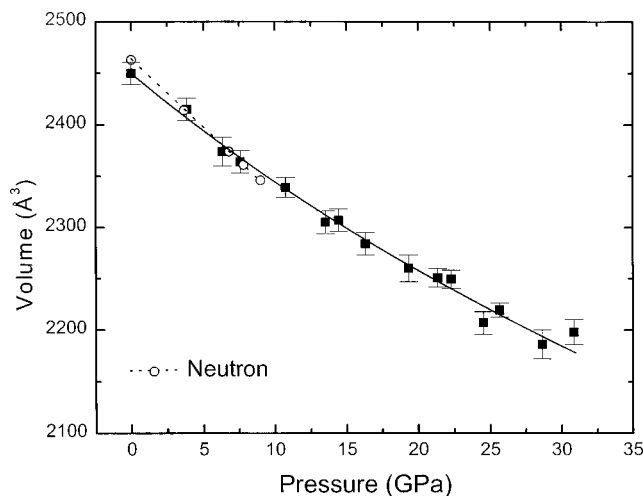


FIG. 3. Equation of state of boron compared with previous work (room temperature, no heating). The error shown on the figure indicates those caused by refinement error of cell parameter and the estimated pressure error of 0.05 GPa.

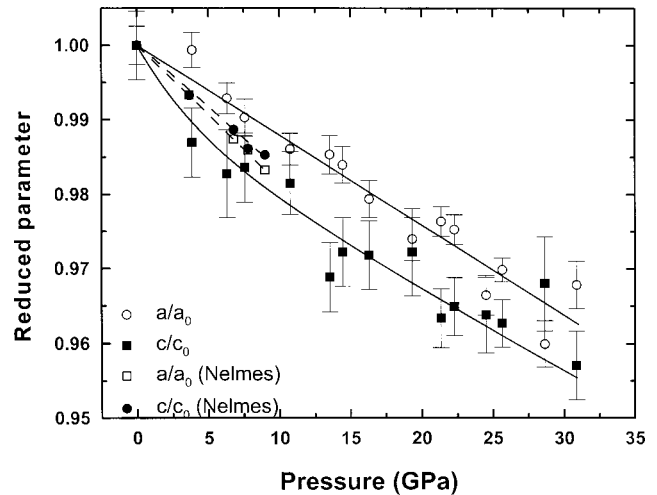


FIG. 4. Pressure dependence of the unit-cell parameter.

GPa below 10 GPa. We found that using a smaller amount of NaCl (or no pressure medium) generates higher anisotropic compression and causes higher experimental error. Our p - V data also indicate that the c/a ratio remains constant at pressures higher than 10 GPa. No phase transformation is observed on room temperature compression. This is consistent with the smooth drop in room-temperature electrical resistivity measured over the pressure range.⁹

B. P - T quench results

Laser-heating experiments were conducted above 10 GPa. At these pressures graphitization of the anvil is avoided because diamond is the stable high-pressure phase. From visible observation after heating at high pressure, we found that the color of the sample is red in transmitted light, and opaque in reflected light. This phenomenon is typical of T -192 boron.² The x-ray diffraction pattern clearly shows a phase transformation compared to that before heating (Fig. 5). To carefully investigate the transition, we prepared several samples using stainless steel, rhenium, and diamond gaskets¹⁶ with different pressure media (NaCl and argon), and measured x-ray diffraction with both the energy dispersive two-dimensional and angle dispersive image plate methods. Figure 6 shows the energy dispersive x-ray diffraction pattern from a temperature-quenched boron sample at 11.7 GPa after heating to 2280 K using the diamond-cell rotation method. The upper part is essentially a three-dimensional plot where the intensities of the x rays are represented by the darkness of the image. The continuous vertical lines are from NaCl, and all short vertical segments are from the boron sample. The lower part of the figure shows the integrated diffraction pattern. The diffraction from the heated sample appears mostly in one 5° step, meaning that the sample recrystallized after heating and became very coarsely crystalline. It can be seen clearly from the step rotation method that we can resolve very weak diffraction in a sample with strong preferred orientation, whereas in the integrated pattern, most of the diffraction lines are not distinguishable. This is an improvement in the high pressure x-ray diffraction tech-

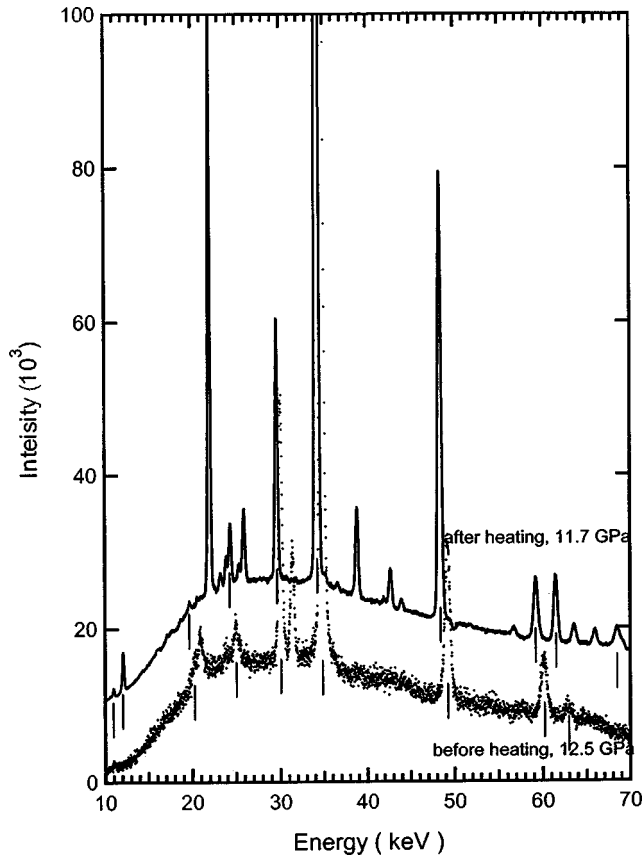


FIG. 5. Comparison diffraction pattern before and after heating at 2280 K. The vertical bar marks the NaCl diffraction peaks, fluorescence and escape peaks. Before heating the pressure measured by ruby was 12.5 GPa. After heating the pressure dropped to 11.7 GPa. NaCl peaks showing higher pressure according to its equation of state, which became comparable after heating.

nique, especially for weakly scattering samples exhibiting significant preferred orientation.

Table I lists the indexed diffraction peaks from a sample examined *in situ* at 11.7 GPa after heated at 2280 K by the energy dispersive method using a diamond gasket. This pattern can be indexed on a tetragonal cell $a=10.058 (\pm 0.006)$, $c=13.77 (\pm 0.02)$ Å, and $V=1393 (\pm 2)$ Å³. The pattern taken by the angle dispersive method for the same sample yields the tetragonal cell parameters $a=10.081 (\pm 0.004)$, $c=13.741 (\pm 0.008)$ Å, and $V=1396 (\pm 2)$ Å³, respectively. The difference is ascribed to the system calibration error for the two different techniques. The pressure-quenched sample can also be refined as a tetragonal structure with cell parameters $a=10.161 (\pm 0.004)$, $c=13.71 (\pm 0.01)$ Å, and $V=1415 (\pm 1)$ Å³ from angle dispersive diffraction data. The calculated density ρ is 2.410(2) g cm⁻³ assuming 190 atoms in the unit cell.

The so-called *T*-192 (or tetragonal II or III or β -tetragonal) phase was first reported by Talley *et al.*¹⁷ by reduction of BBr₃ on hot tungsten and other metals at temperatures from 1543 to 1823 K. The cell parameters were also given as $a=10.12 (\pm 0.01)$, $c=14.17 (\pm 0.01)$, and $V=1457.3$ Å³ for a CVD grown sample.¹⁸ These are consistent with our experimental results. The slight difference is prob-

ably due to the residual stress in the sample upon recovery from high pressure. The diffraction obtained with an argon pressure medium give refined cell parameters of $a=10.10 (\pm 0.02)$, $c=13.62 (\pm 0.03)$ Å, $V=1388 (\pm 4)$ Å³, and $\rho=2.364 (\pm 0.004)$ g cm⁻³ at 12.4 GPa, consistent with the NaCl medium results within the error range. This comparison allows us to eliminate the possibility that the transformation arises from boron reacting with other elements. The results are consistent with the transformation of *R*-105 boron to the quenchable *T*-192 form after high-pressure/high-temperature processing.

We examined *R*-105 boron at higher pressures and similar temperature, and quenched the sample to ambient conditions for x-ray diffraction measurements. Over the pressure range studied (to 30.7 GPa), the phase undergoes a high *P-T* transformation. Our results further indicate that the transformation boundary has a negative *P-T* slope. The phase thus appears to be both a high-pressure (high density) and high-temperature (high entropy) phase. Earlier experiments² show that when *T*-192 boron is heated at ambient pressure, the rhombohedral modification appears, indicating that the tetragonal form is not a stable phase under ambient conditions. If the transformation occurs at higher pressure at room temperature, the transition may be responsible for the change in electrical resistivity found near 35 GPa and 300 K (Ref. 10).

C. Implications for bonding changes

An examination of the bonding properties of boron phases provides insight into the present observations. The *P-V* work (to 30.7 GPa) is not sufficient to drive cluster fragmentation, even at high temperature (cf. Ref. 11). The *R*-105 rhombohedral unit cell can be considered as consisting of one B84-(B10-B-B10) chemical unit. The B84 unit is actually a B12-12B6 unit, i.e., one B12 icosahedron directly bonded to 12 other half B12 icosahedra in the unit cell. The B10 unit may be derived from condensation of three B12 icosahedra around a threefold axis of the cell^{2,19} [see Fig. 7(a)]. It is located among three nearest B12 icosahedra, sharing bonds with them to form a three-dimensional framework in which all boron atoms are a part of an icosahedron. We recognize this as the more extended B12 icosahedral framework. The *T*-192 structure, however, contains four B21-2B12-B2.5 units. Each B12 icosahedron is directly linked to six adjacent B12 icosahedra, five B21 twinned icosahedra and one single boron atom.¹⁷ Instead of forming a bond with a B10 cluster through the half icosahedron in the *T*-105 structure, the B12 icosahedron forms a bond with B21 clusters. The B21 unit in the *T*-192 structure is a twinned icosahedron, with three common atoms on a shared triangle of the icosahedra [Fig. 7(b)].^{2,17} This provides a mechanism for producing a denser structure starting with the long-range icosahedral framework in *R*-105 boron.

Two B10 clusters and one single atom form a B10-B-B10 chain in the rhombohedral phase. One atom from a B10 unit is shared by three B84 clusters and six others are shared by two of the B84 clusters. The three unshared atoms are bonded to one atom at the center of the chain. Our compressibility data for *R*-105 shows that the *a* axis is more rigid than

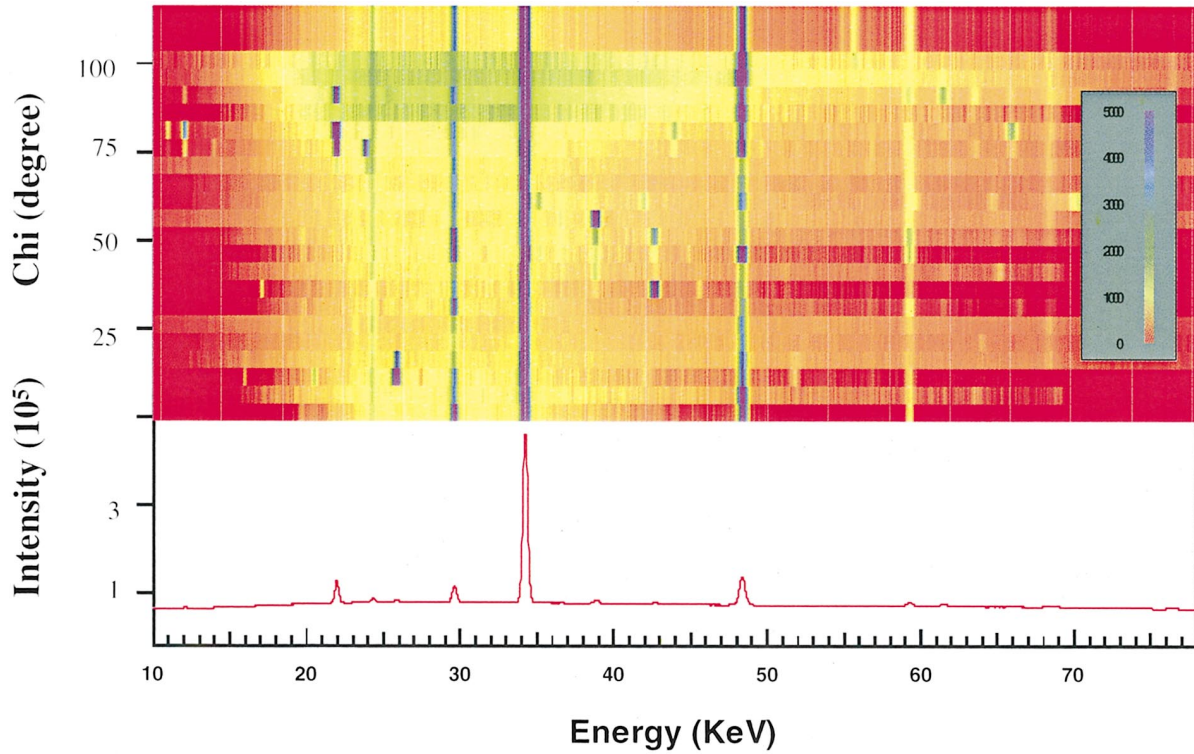


FIG. 6. (Color) Step-rotated x-ray diffraction image with an integrated pattern of boron in NaCl at 11.7 GPa. Top: the image of diffraction within a 100° χ rotation; lower: calculated pattern from boron T-192 structure with the cell parameter refined from the data at 11.7 GPa, middle: the black bar indicates the position of NaCl and the escaped line.

the c axis (hexagonal setting) below 10 GPa. The c -axis corresponds to the $[111]$ direction of the rhombohedral setting along with the B10-B-B10 chain direction (threefold axis). The results show that the B10-B-B10 chain is softer than the

B84-B84 chain under pressure, a condition that may lead to icosahedra twinning on compression. Unlike in the R -105 structure where the B21 cluster forms one bond with each of the three half icosahedra of the B84 chain, the B21 cluster in

TABLE I. EDXRD pattern of T -quenched born at 11.7 GPa with refinement cell symmetry: tetragonal $a = 10.058(\pm 0.006)$, $c = 13.72(\pm 0.02)$, and $V = 1393(\pm 2)$.

hkl	d	d (calc)	d (diff.)	hkl	d	d (calc.)	d (diff.)
2 0 0	5.169	5.029	0.140	6 0 1	1.662	1.664	-0.002
1 2 1	4.282	4.276	0.006	3 5 3	1.613	1.615	-0.002
2 0 2	4.030	4.061	-0.031	6 2 0	1.592	1.590	0.002
2 2 1	3.498	3.443	0.055	5 4 1	1.562	1.561	0.001
0 0 4	3.438	3.442	-0.004	5 1 6	1.495	1.496	-0.001
4 0 0	2.508	2.514	-0.006	4 5 3	1.484	1.486	-0.002
2 0 5	2.422	2.415	0.007	6 2 4	1.441	1.444	-0.003
4 0 2	2.366	2.362	0.004	7 1 2	1.395	1.393	0.002
1 4 2	2.301	2.299	0.002	7 2 0	1.384	1.382	0.002
1 0 6	2.282	2.237	0.045	7 0 3	1.369	1.371	-0.002
4 1 3	2.155	2.154	0.001	6 4 2	1.361	1.367	-0.006
3 3 3	2.110	2.106	0.004	6 1 6	1.343	1.342	0.001
3 1 5	2.076	2.082	-0.006	4 6 3	1.334	1.334	0.000
4 3 0	2.015	2.012	0.003	5 1 8	1.296	1.297	-0.001
3 4 2	1.942	1.931	0.011	2 2 10	1.282	1.284	-0.002
4 4 0	1.787	1.778	0.009	8 0 0	1.257	1.257	0.000
5 3 0	1.731	1.725	0.006	8 3 2	1.160	1.160	0.000
6 0 0	1.677	1.676	0.001				

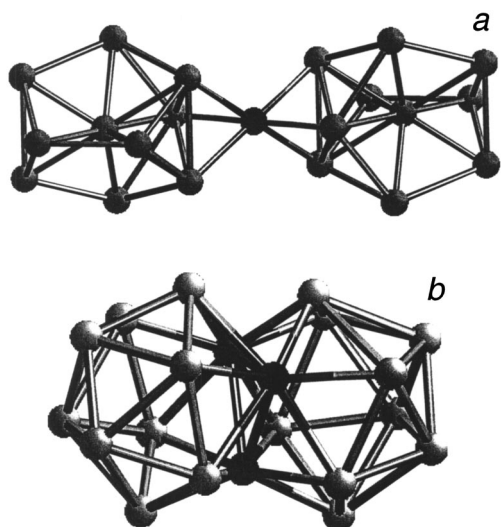


FIG. 7. Schematic diagram of the B21 cluster of boron in different unit cells: (a) B21 as a chain in the R-105 unit cell, and (b) B21 as twinned icosahedra in the T-192 unit cell.

the *T*-192 structure forms only one bond with the B12 cluster, indicating that inter-cluster bonding is weakened at high pressure. Detailed structure refinements (e.g., based on single crystal diffraction) are required to confirm this picture.

IV. CONCLUSIONS

We have investigated the compressibility of *R*-105 boron to 30.7 GPa and determined a bulk modulus of 205 (± 16) GPa. We found that the *a* direction of *R*-105 boron (hexagonal setting) is less compressible than *c*, which indicates that the B10-B-B10 chain is less rigid than the B12 cluster. We have also demonstrated that boron transforms to a tetragonal phase at pressures higher than 10 GPa after heating at temperatures higher than 1500 K. The results suggest that the phase is the previously established *T*-192 phase, or one closely related to it. The negative *P-T* slope on transformation from B-105 (in the absence of other transitions) indicates that the phase is both a high density and high entropy phase. We ascribe the transformation to both intercluster bonding adjustments around the B12 unit and the deformation of the B21 unit, and point toward an increasing role of multicenter bonding in boron in this range of pressures.

ACKNOWLEDGMENTS

We thank C. S. Zha at CHESS and J. Hu at NSLS for technical support in synchrotron x-ray diffraction measurements, and M. I. Erements for useful discussions. This work was supported by the NSF, the DOE, and Basic Research project of the MOST of China.

-
- ¹D. Emin, *Phys. Today* **40** (1), 55 (1987).
²J. Donohue, *The Structure of the Elements* (Krieger, Malabar, FL, 1982), Chap. 5, pp. 48–82.
³E. Amberger and K. Ploog, *J. Less-Common Met.* **23**, 21 (1971).
⁴P. W. Bridgman, *Proc. Am. Acad. Arts Sci.* **64**, 75 (1930).
⁵R. H. Wentorf, Jr., *Science* (Washington, DC, U.S.) **147**, 49 (1965).
⁶R. J. Nelmes, J. S. Loveday, D. R. Allan, J. M. Besson, G. Hamel, P. Grima, and S. Hull, *Phys. Rev. B* **47**, 7668 (1993).
⁷R. J. Nelmes, J. S. Loveday, R. M. Wilson, W. G. Marshall, J. M. Besson, S. Klotz, G. Hamel, T. L. Aselage, and S. Hull, *Phys. Rev. Lett.* **74**, 2268 (1995).
⁸R. Lazzari, N. Vast, J. M. Besson, S. Baroni, and A. Dal Corso, *Phys. Rev. Lett.* **83**, 3230 (1999).
⁹N. Vast, S. Baroni, G. Zerah, J. M. Besson, A. Polian, M. Grimsditch, and J. C. Chervin, *Phys. Rev. Lett.* **78**, 693 (1996).
¹⁰M. I. Erements, V. V. Struzhkin, H. K. Mao, and R. J. Hemley, *Science* (Washington, DC, U.S.) **293**, 272 (2001).
¹¹C. Mailhot, J. B. Grant, and A. K. McMahan, *Phys. Rev. B* **42**, 9033 (1990).
¹²J. Hu, H. K. Mao, J. F. Shu, and R. J. Hemley, in *High-Pressure Science and Technology-1993*, edited by S. C. Schmidt, J. W. Shaner, G. A. Samara, and M. Ross, (AIP, New York, 1994).
¹³G. Shen, H. K. Mao, and R. J. Hemley, in *Advanced Materials '96—New Trends in High Pressure Research* (NIRIM, Tsukuba, Japan, 1996), p. 149.
¹⁴H. K. Mao, G. Shen, R. J. Hemley, and T. S. Duffy, in *Properties of the Earth and Planetary Materials at High Pressures*, edited by M. H. Manghnani and T. Yagi (AGU, Washington, DC, 1998), p. 27.
¹⁵Y. Ma, H. K. Mao, R. J. Hemley, S. A. Gramsch, G. Shen, and M. Somayazulu, *Rev. Sci. Instrum.* **72**, 1302 (2001).
¹⁶G. T. Zou, Y. Ma, H. K. Mao, R. J. Hemley, and S. A. Gramsch, *Rev. Sci. Instrum.* **72**, 1298 (2001).
¹⁷C. P. Talley, S. LaPlaca, and B. Post, *Acta Crystallogr.* **13**, 271 (1960).
¹⁸M. Vlasse, R. Naslain, J. S. Kasper, and K. Ploog, *J. Solid State Chem.* **28**, 289 (1979).
¹⁹J. L. Hoard, D. B. Sullenger, C. H. L. Kennard, and R. E. Hughes, *J. Solid State Chem.* **1**, 268 (1970).